



RESEARCH ARTICLE

Persistent increase in ventral hippocampal long-term potentiation by juvenile stress: A role for astrocytic glutamine synthetase

Sebastian Ivens^{1,2} | Gürsel Çalışkan^{2,3,4} | Ismini Papageorgiou^{5,6}  |
Tiziana Cesetti^{5,7} | Ansgar Malich⁶ | Oliver Kann⁵ | Uwe Heinemann² |
Oliver Stork^{3,4} | Anne Albrecht^{3,4} 

¹Department of Psychiatry and Psychotherapy, Charité-Universitätsmedizin Berlin, Berlin, Germany

²Institute for Neurophysiology, Charité-Universitätsmedizin Berlin, Berlin, Germany

³Institute of Biology, Otto-von-Guericke-University Magdeburg, Magdeburg, Germany

⁴Center for Behavioral Brain Sciences, Magdeburg, Germany

⁵Institute of Physiology and Pathophysiology, University of Heidelberg, Heidelberg, Germany

⁶Institute of Radiology, Suedharz Hospital Nordhausen, Nordhausen, Germany

⁷Institute of Molecular and Cell Biology, University of Applied Sciences Mannheim, Mannheim, Germany

Correspondence

Anne Albrecht, Department of Genetics & Molecular Neurobiology, Institute of Biology, Otto-von-Guericke-University Magdeburg, Leipziger Str. 44, 39120 Magdeburg, Germany. Email: anne1.albrecht@ovgu.de

Funding information

German Research foundation, Grant/Award Number: CRC779 TPB5; European fund for regional development (EFRE), Grant/Award Number: ZS/2016/04/78113; Excellence cluster NeuroCure; German Israeli Project Cooperation, Grant/Award Number: He1128/16-1; Leibniz-Gemeinschaft, Grant/Award Number: SAS-2015-LIN-LWC

Abstract

A traumatic childhood is among the most important risk factors for developing stress-related psychopathologies such as posttraumatic stress disorder or depression later in life. However, despite the proven role of astrocytes in regulating transmitter release and synaptic plasticity, the contribution of astrocytic transmitter metabolism to such stress-induced psychopathologies is currently not understood. In rodents, childhood adversity can be modeled by juvenile stress exposure, resulting in increased anxiety, and impaired coping with stress in adulthood. We describe that such juvenile stress in rats, regardless of additional stress in adulthood, leads to reduced synaptic efficacy in the ventral CA1 (vCA1) Schaffer collaterals, but increased long-term potentiation (LTP) of synaptic transmission after high-frequency stimulation. We tested whether the glutamate–glutamine-cycle guides the lasting changes on plasticity observed after juvenile stress by blocking the astrocytic glutamate-degrading enzyme, glutamine synthetase (GS). Indeed, the pharmacological inhibition of GS by methionine sulfoximine in slices from naïve rats mimics the effect of juvenile stress on vCA1-LTP, while supplying glutamine is sufficient to normalize the LTP. Assessing steady-state mRNA levels in the vCA1 *stratum radiatum* reveals distinct shifts in the expression of GS, astrocytic glutamate, and glutamine transporters after stress in juvenility, adulthood, or combined juvenile/adult stress. While GS mRNA expression levels are lastingly reduced after juvenile stress, GS protein levels are maintained stable. Together our results suggest a critical role for astrocytes and the glutamate–glutamine cycle in mediating long-term effects of juvenile stress on plasticity in the vCA1, a region associated with anxiety and emotional memory processing.

KEYWORDS

astrocytes, glutamate–glutamine cycle, glutamine synthetase, juvenile stress, LTP, ventral hippocampus

Sebastian Ivens and Gürsel Çalışkan should be considered joint first author.

This is an open access article under the terms of the Creative Commons Attribution License, which permits use, distribution and reproduction in any medium, provided the original work is properly cited.

© 2019 The Authors. GLIA published by Wiley Periodicals LLC



1 | INTRODUCTION

Stress is a common experience in our daily life. While the central nervous system is usually set to efficiently cope with stress, stress adaptation fails under certain circumstances and long-lasting alterations in anxiety, mood, and cognition are observed (Koolhaas et al., 2011). However, in spite of ample insights into the astrocytic regulation of neural plasticity (e.g., Dallérac, Zapata, & Rouach, 2018), it is still not understood how these processes are involved in adaptive and maladaptive long-term effects of stress exposure.

Epidemiological studies suggest childhood adversity as a prominent predisposing factor for developing depression and anxiety disorders later in life (Heim & Nemeroff, 2001; McLaughlin et al., 2010). We and others therefore started to investigate the neurobiological correlates of childhood adversity, using a rodent model that utilizes variable, unpredictable stress exposure in the postweaning to prepubertal life phase (see Albrecht et al., 2017, for review). Pre-exposure to such “juvenile stress” can increase anxiety-like behavior and, just like in humans, heightens the prevalence for increased adverse emotional responses following traumatic stress in adulthood (Ardi, Albrecht, Richter-Levin, Saha, & Richter-Levin, 2016; Avital & Richter-Levin, 2005). Similarly, previous exposure to juvenile stress increases fear memory and its generalization after fear conditioning (Müller, Obata, Richter-Levin, & Stork, 2014; Yee, Schwarting, Fuchs, & Wöhr, 2012) and reduces active stress coping in aversive shuttle box learning in adulthood (Horovitz, Tsoory, Hall, Jacobson-Pick, & Richter-Levin, 2012). Such a combination of juvenile stress and consecutive aversive learning paradigms serving as stress in adulthood is particularly effective in lastingly enhancing anxiety- and depression-like behaviors (Gruber et al., 2015; Horovitz et al., 2012; Müller et al., 2014). The behavioral phenotype induced by juvenile stress and its combination with adult stress has drawn the attention toward the ventral hippocampus, a brain structure closely involved in fear memory and anxiety (Bannerman et al., 2004). Juvenile stress exposure and its combination with adult stress promotes the formation and increases the maintenance of long-term potentiation of synaptic plasticity (LTP) in the ventral hippocampal CA1, while rather decreasing LTP in the dorsal CA1 (Grigoryan, Ardi, Albrecht, Richter-Levin, & Segal, 2015; Maggio & Segal, 2011). While the ventral hippocampus is rather associated with emotional stimulus processing, the dorsal part plays a major role in cognitive tasks such as spatial navigation and memory (Fanselow & Dong, 2010). A history of juvenile stress has been suggested to increase plasticity in the ventral hippocampal system, thereby favoring emotional stimulus processing and promoting fear and anxiety later in life (Segal, Richter-Levin, & Maggio, 2010).

Emerging evidence suggests a putative role of altered GABAergic function (Ardi et al., 2016; Müller et al., 2014; see also Albrecht et al., 2017, for review), but especially for lastingly modulating LTP following juvenile stress, astrocytes comprise an interesting target. Using state-of-the-art chemogenetic tools, a recent study demonstrated that astrocytic activation enhances and even induces LTP in the CA1 region of the hippocampus and increases also memory strength

(Adamsky et al., 2018; see also Allen & Lyons, 2018). Upon induction of LTP, glutamate is released and binds to specific ionotropic receptors (NMDA and AMPA subtype) as well as metabotropic receptors, leading ultimately to the restructuring of synapses and a lastingly optimized signal transduction at potentiated synapses (Baltaci, Mogulkoc, & Baltaci, 2018; Larson & Munkácsy, 2015). Astrocytes can modulate LTP by regulating glutamate levels at the synapse and by releasing cofactors of glutamate receptors at neurons. Glutamate is taken up into astrocytes via specific transporters like glutamate transporter 1 (GLT-1), thereby supporting termination of excitatory neuronal signaling and preventing neurotoxic effects of excess glutamate. Glutamate is metabolized to glutamine by the enzyme glutamine synthetase within astrocytes; glutamine is then shuttled back to neurons, which use glutaminase to synthesize new glutamate. In inhibitory neurons, glutamate is further converted to the inhibitory neurotransmitter γ -aminobutyric acid (GABA) via glutamate decarboxylase (GAD65/67) (Rose, Verkhratsky, & Parpura, 2013).

The glutamate–glutamine cycle in astrocytes appears to be adjusted depending on neuronal activity and sets the threshold for regional excitability and plasticity (Bonansco et al., 2011; Rose et al., 2013; Tani et al., 2014; Trabelsi, Amri, Becq, Molinari, & Aniksztejn, 2017). In the current study, we set out to investigate the contribution of the glutamate–glutamine cycle in astrocytes to alter LTP as a consequence of juvenile stress exposure. We utilized the pharmacological blockage of the astrocytic key enzyme of the glutamate–glutamine cycle, glutamine synthetase, and found that such a treatment mimicked the augmenting effect of juvenile stress on ventral CA1 (vCA1) LTP. Overcoming the functional glutamine synthetase deficit after juvenile stress by external administration of glutamine normalized LTP. We further investigated steady-state mRNA levels for the different components of the glutamate–glutamine cycle and found complex expression shifts in the vCA1 *stratum radiatum* after juvenile stress, adult stress, or the combination of both. Together, our results indicate that astrocytes and their contribution to the glutamate–glutamine cycle is lastingly affected by stress exposure and contributes to the allostatic regulation of long-term plasticity, especially after juvenile stress.

2 | METHODS

2.1 | Animals

Male Wistar rats obtained from Harlan (Germany) at postnatal day (PND) 21 were used for all experiments, in accordance with the European and German regulations for animal experiments and were approved by the local authorities (LAGESO, T0068/02 and G0397/09). Housing in groups of 4–6 rats per cage; 12 hr light–dark cycle, lights on at 7 a.m.; room temperature $22 \pm 2^\circ\text{C}$.

2.2 | Behavioral manipulations

After 1 week of acclimatization and handling, rats were exposed to “juvenile stress” (JS) as described before (Albrecht et al., 2016), by receiving 15 min of forced swim on PND 27, three 30 min sessions of

elevated platform (Inter-Trial Interval [ITI]: 60 min in the home cage) on PND 28 and 2 hr of restraint on PND 29. At PND 60, the rats were exposed to one session of two-way shuttle avoidance training (*adult stress, AS*; Albrecht et al., 2016), consisting of 100 trials, each with a tone as conditional stimulus (maximal duration 10 s), immediately followed by a footshock (0.8 mA, for maximum of 10 s; ITIs randomly varying with 60 ± 12 s). After such combined JS + AS exposure, rats were left undisturbed for 14 days in their home cage until brain preparation took place. Additional groups of animals were exposed to either only JS or only AS, a control group (C) was handled only and received no AS or JS.

2.3 | Electrophysiology

2.3.1 | Slice preparation

On PND 74, all rats were decapitated after anesthesia with a isoflurane-dinitrogen oxide (N_2O) mixture. Their brains were rapidly removed and placed in cold (4–8°C) carbogenated (5% $CO_2/95\% O_2$) artificial cerebrospinal fluid (aCSF, composition in mM: 129 NaCl, 21 $NaHCO_3$, 3 KCl, 1.6 $CaCl_2$, 1.8 $MgSO_4$, 1.25 NaH_2PO_4 , 10 glucose). Transverse-like ventral hippocampal slices (400 μm) were obtained by cutting horizontal brain sections including the ventral pole of the hippocampus on an angled platform ($\sim 12^\circ$). Three-to-four ventral slices per hemisphere were transferred to an interface chamber perfused with aCSF at $36 \pm 0.2^\circ C$ (flow rate: 1.8 ± 0.2 mL/min, pH 7.4, osmolarity ~ 300 mOsmol/kg) and incubated at least for 90 min before starting recordings.

2.3.2 | Data acquisition

Extracellular field recordings were obtained by placing a glass electrode filled with aCSF (1–3 M Ω) at the dendritic layer of the CA1 region (*stratum radiatum*) at 70–100 μm depth and by stimulating the Schaffer collaterals with a bipolar platinum wire electrode with exposed tips of 50–80 μm (tip separations ~ 100 μm ; electrode resistance in aCSF ~ 10 k Ω) placed at the proximal *stratum radiatum* of CA1 (Figure 1a). Signals were preamplified using a custom-made amplifier equipped with negative capacitance regulation, low-pass filtered at 3 kHz and sampled at a frequency of 10 kHz using Signal software (Version 4, Cambridge Electronic Design [CED], Cambridge, UK) and stored on a computer hard disc for off-line analysis using a CED 1401 interface (CED, Cambridge, UK).

2.3.3 | Stimulation protocols

After recording 20–30 min of baseline responses (0.033 Hz, pulse duration: 100 μs), an input–output (I–O) curve was obtained by using seven intensities ranging from 1 to 5 Volts (V). The stimulus intensity that resulted in 50% of the maximum amplitude was further used for long-term potentiation (LTP) experiments. After recording a second baseline for 12.5 min, LTP was induced using a single train of

100 pulses for 1 s (100 Hz). After LTP induction, responses were recorded for 40 min (0.033 Hz).

2.3.4 | Drugs and application protocol

Slices of control and stress-exposed rats were perfused with aCSF (C: number of slices, $n = 10$ /number of animals, $N = 6$; JS: $n = 10/N = 8$; AS: $n = 9/N = 5$; JSAS: $n = 11/N = 7$). In separate slices, 1.5 mM methionine sulfoximine (MSO; Sigma-Aldrich, Germany) was added to the aCSF 90 min before the first baseline (C: $n = 15/N = 7$; JS: $n = 11/N = 7$; AS: $n = 8/N = 5$; JSAS: $n = 11/N = 6$). In additional slices of the control and JS group, 1 mM glutamine (Gln; Sigma-Aldrich, Germany; C: $n = 14/N = 8$; JS: $n = 13/N = 6$) or a combination of MSO and Gln (C: $n = 10/N = 6$) was included in aCSF again 90 min before the first baseline and recordings of I–O curve and LTP commenced as described above.

2.3.5 | Data analysis and statistics

Evoked potentials were analyzed using MATLAB- (MathWorks, Natick, MA) and Spike2-based analysis tools (CED, Cambridge). The slope of fEPSPs were analyzed by calculating the slope (V/s) between the 10 and 90% of the fEPSP amplitudes. The fiber volley (FV) amplitude was measured by calculating the peak-to-peak amplitude of the descending phase of the FV. To analyze the efficacy of synaptic transmission, the slope of the postsynaptic fEPSP was divided by the amplitude of the corresponding presynaptic FV as previously published by us and others (Figure 1b; Annamneedi et al., 2018; Chen, Kagan, Hirakura, & Xie, 2000; Nguyen, Abel, Kandel, & Bourtschouladze, 2000; Patterson et al., 1996).

The effect of stress groups (juvenile and adult stress main effects), drug application and their interaction on fEPSP slopes, FV amplitudes and the fEPSP slope to FV amplitude ratios over increasing stimulation intensities during measurement of I–O curves were determined using repeated measure ANOVA. If necessary, Greenhouse–Geisser corrections were applied for sphericity issues. For LTP analysis, the data was normalized to the average of 12.5 min baseline before induction. Main effects of juvenile and adult stress and of the drugs applied within the different stress groups were determined in the normalized average responses of the last 5 min of recordings with Mann–Whitney *U* test, as the data was not normally distributed (tested with Shapiro–Wilk test).

2.4 | mRNA expression

2.4.1 | Brain preparation and laser capture microdissection

At PND 74 rats of all four groups ($n = 6$ – 7 each) were sacrificed, their brains were quickly removed from the skull, snap-frozen in methylbutane cooled by liquid nitrogen, and stored at $-80^\circ C$. About 20 μm thick horizontal sections of the ventral hippocampus (-6.3 until -6.8 mm from Bregma; Paxinos & Watson, 1998) were cut on a cryostat and thaw-mounted on poly-L-lysine coated RNase-free membrane slides. After fixation in $-20^\circ C$ cold ethanol and a brief cresyl

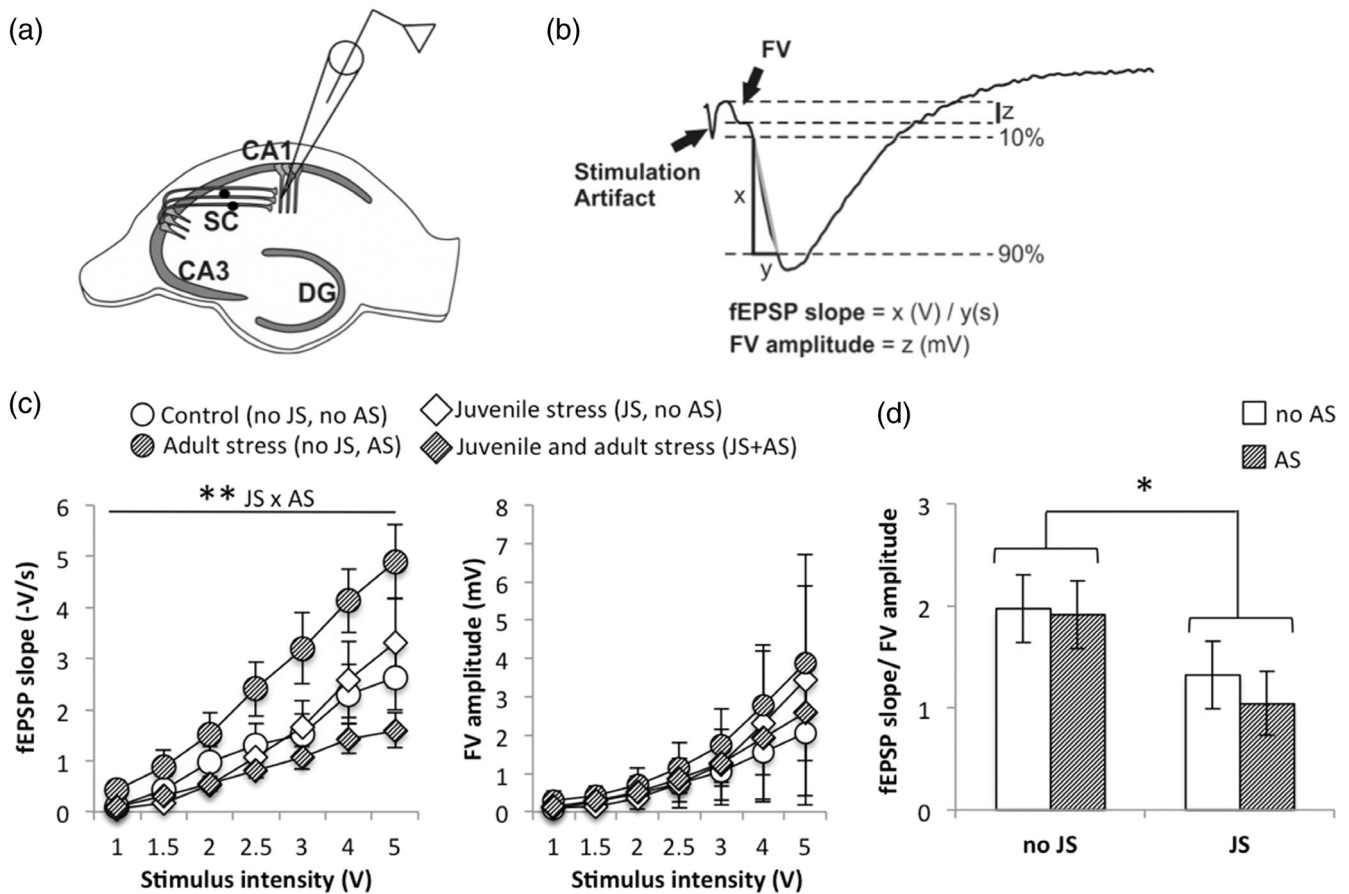


FIGURE 1 Juvenile stress reduces synaptic efficacy. For electrophysiological recordings in the ventral Schaffer collateral (SC)-CA1 synapses, the recording electrode was positioned at the *stratum radiatum* of the vCA1, while a bipolar stimulation electrode was placed in the proximal *stratum radiatum* (two black dots) to stimulate SC (a). SC stimulation elicited a typical response consistent of a presynaptic fiber volley (FV) followed by a postsynaptic field potential (fEPSP). The FV amplitude was calculated via measuring the peak-to-peak amplitude of the descending phase. The slope was calculated by using the 10 and 90% data points of the maximum EPSP amplitude (depicted as gray line). Calculating the ratio of fEPSP slope and FV serves as a measure for the synaptic transmission efficacy (b). A previous history of juvenile (JS) and adult stress (AS) modified the fEPSP slope (c, left panel), but not the FV (c, right panel) response over increasing stimulation intensities during input-output-curve measures. While a single stress experience in adulthood (AS) or juvenility (JS) increased the fEPSP slope response, rather a reduction was observed in animals stressed twice in juvenility and adulthood (JS + AS). However, synaptic transmission efficacy, determined by presynaptic and postsynaptic response ratios (averaged over all stimulation intensities), was reduced by JS, regardless of an additional adult stressor (d). All values are mean \pm SEM. *Significant effect of stress exposure (JS or the interaction of JS \times AS), $p < .05$; ** $p < .01$

violet acetate staining under nuclease-minimized conditions, the *stratum radiatum* of the vCA1 was microdissected from 8 to 10 sections per animal using a laser microbeam dissection system (Carl Zeiss, Jena, Germany) and collected in an adhesive cap capture device.

2.4.2 | Reverse transcription and real-time PCR

Lysis and isolation total RNA was done using the RNeasy Micro Plus kit (Qiagen, Hilden, Germany) according to manufacturer's instructions, including steps for removal of genomic DNA. First-strand cDNA was synthesized using 2.5 mM dNTPs, 50 μ M Oligo (dT) 18 and 50 μ M random decamer first strand primers (Life Technologies, Darmstadt, Germany) as well as RNase Inhibitor (SuperaseIN; 20 U/ μ L; Life Technologies, Darmstadt, Germany) with the Sensiscript Reverse Transcription kit (Qiagen, Hilden, Germany; 60 min at 37°C). Multiplex Real time PCR was performed using the ABI Prism Step One real time PCR

apparatus (Life Technologies, Darmstadt, Germany) and TaqMan[®] reagents with predesigned assays for the target genes (assay IDs: Glul: Rn01483107_m1; GLS: Rn00561285_m1; GLT-1: Rn00691548_m1; SN1: Rn01447660_m1; GAT-3: Rn00577664_m1) and for the house-keeping gene glyceraldehyd-3-phosphat-dehydrogenase (GAPDH; endogenous control, Life Technologies, Darmstadt, Germany) with 1:5 dilutions of cDNA, run in triplicates with 50 cycles of 15 s at 95°C and 1 min at 60°C, preceded by a 2 min 50°C decontamination step with uracil-N-glycosidase and initial denaturation at 95°C for 10 min.

2.4.3 | Data analysis and statistics

For relative quantification (RQ) via the ddCT method, the mean cycle threshold (CT) of each triplicate assay was first normalized to the overall content of cDNA using GAPDH as an internal control (dCT; dCT[target gene]) = (CT [target gene]) - (CT [GAPDH]) and then to the control group

with $ddCT = dCT(\text{sample}) - \text{mean } dCT(\text{control group})$. By applying the formula $RQ\% = (2^{-ddCT}) \times 100$, RQ values for a specific target gene were obtained. Following Shapiro–Wilk test for normality, main effects of JS or AS were assessed with Mann–Whitney U test in non-normal distributed samples. In normally distributed data sets JS and AS effects as well as their interaction were analyzed by a two-way ANOVA.

2.5 | Glutamine synthetase immunohistochemistry

2.5.1 | Tissue fixation and slicing

Three control and three juvenile stressed rats were perfused transcardially with phosphate buffered 4% paraformaldehyde solution at pH 6.8, as previously described (Albrecht et al., 2016). After post-fixation overnight in the same fixative at 4°C, brains were prepared for cryoslicing with an overnight immersion in wt/vol 20% sucrose vol/vol 10% glycerine solution. About 30 μm thick, serial horizontal hippocampal sections from each animal were stored free-floating in a 40% ethylene glycol-based antifreeze solution.

2.5.2 | GS staining

Immunohistochemical staining for glutamine synthetase with a mouse monoclonal anti-glutamine synthetase antibody (Millipore) and diaminobenzidine development for light microscopy followed as previously reported (Papageorgiou, Gabriel, Fetani, Kann, & Heinemann, 2011), with a primary antibody dilution of 1:1,000 in 10% normal goat serum and secondary antibody dilution 1:2,000 in 0.2% bovine serum albumin.

2.5.3 | Design-based stereology and optical fractionator

For design-based stereological estimation of the total GS-expressing cell number in the CA1 *stratum radiatum*, we sampled $n = 7$ slices per animal at the level of the ventral hippocampus (−6.3 until −6.8 mm from Bregma; Paxinos & Watson, 1998). The optical fractionator was implemented with a Uniform Random Grid of $120 \times 120 \mu\text{m}$, a fractionator sampling frame of $45 \times 45 \mu\text{m}$ and a fractionator height of 15 μm . The postprocessing section thickness was measured during counting in every fifth sampling site and the estimated cell number was corrected for the initial slice thickness (30 μm). The average coefficient of error (CE) of the number estimator was 0.08 ± 0.02 for both groups.

2.5.4 | Densitometry

The GS protein expression level was semiquantitative analyzed in the same sections used for stereological analysis with gray densitometry. $N = 21$ (seven triplets) of $\times 40$ magnified CA1 *stratum radiatum* images per animal from the ventral hippocampal segment, acquired with the same filtering and exposure time settings were used for this purpose. The raw intensity histograms were extracted from 8/bit grayscale images and each was quantified in terms of the AUC and the dominating gray

intensity, defined as the gray intensity value with the maximum pixel number. Mean values were then calculated for each animal.

2.5.5 | Statistical analysis and halftones

Data were treated as unpaired. Groups were compared with a two-tailed Student's t test after testing for normal distribution with the Shapiro–Wilk test. Halftones were composed with CorelDRAW Graphics Suite X6 (Corel GmbH, Munich, Germany). The tone curve and brightness of microphotographs have been adjusted only for demonstration purposes.

3 | RESULTS

3.1 | Juvenile stress reduces synaptic efficacy

The impact of juvenile and adult stress on basal synaptic transmission at the ventral Schaffer collateral (SC) - CA1 synapse was analyzed by recording I–O curves. While the fEPSP slope describes postsynaptic responses at the dendritic level, the FV amplitude indicates synchronous firing of presynaptic neurons upon stimulation (Figure 1b). Repeated measure ANOVA (with Greenhouse–Geisser correction) indicated a significant interaction of juvenile and adult stress over the range of seven different stimulation intensities from 1 to 5 V on the fEPSP slope ($F[1.488,99.678] = 8.876, p = .001$), suggesting that combined exposure to juvenile and adult stress induces a less steep increase in fEPSP slope under high stimulation intensities than a stressor either in juvenility or adulthood separately (Figure 1c). A trend for an interaction of juvenile and adult stress was observed over increasing stimulation intensities for the FV amplitude as well (Figure 1c; $F[1.142,73.107] = 3.473, p = .061$). After wash-in of MSO a similar interaction of juvenile and adult stress was observed for the fEPSP slope (Figure S1a left; $F[1.393,51.542] = 4.09, p = .036$), but not for the FV amplitude (Figure S1a right; $F[1.143,39.996] = 0.694, p = .428$). Calculating the ratio of these measures, fEPSP slope normalized by FV amplitude, allows determining the efficacy of synaptic transmission. Here, a main effect of juvenile stress was observed that was independent of any additional exposure to adult stress (Figure 1d, averaged over stimulation intensities; $F[1,29] = 5.405, p = .027$). The same effect was visible under blockage of glutamine synthetase, although here only in trend (Figure S1b; $F[1,33] = 3.701, p = .063$), as MSO wash-in increased the variability of the measurements (see increased standard error of mean, Figure 1d vs. Figure S1b).

Together, while combined juvenile and adult stress had a differential effect on regulating presynaptic and postsynaptic baseline stimulation responses, juvenile stress per se reduced basal synaptic transmission efficacy at the vCA1-SC synapse that appears rather independent of glutamine synthetase activity.

3.2 | Increased vCA1-LTP after juvenile stress is mimicked by a glutamine synthetase blocker

We then investigated the role of glutamine synthetase on the lasting impact of juvenile stress, with and without additional adult stress

exposure, on vCA1-LTP in slices obtained from rats that had undergone differential stress exposure (Figure 2a–d). In accordance with previous studies, LTP in the vCA1 is relatively small in control slices,

but exposure to juvenile stress increased LTP lastingly and independently from additional adult stress (Figure 2e; main effect of JS: $U[40] = 2.803$, $p = .004$; AS: $U[40] = 1.055$, $p = .301$). Wash-in of the

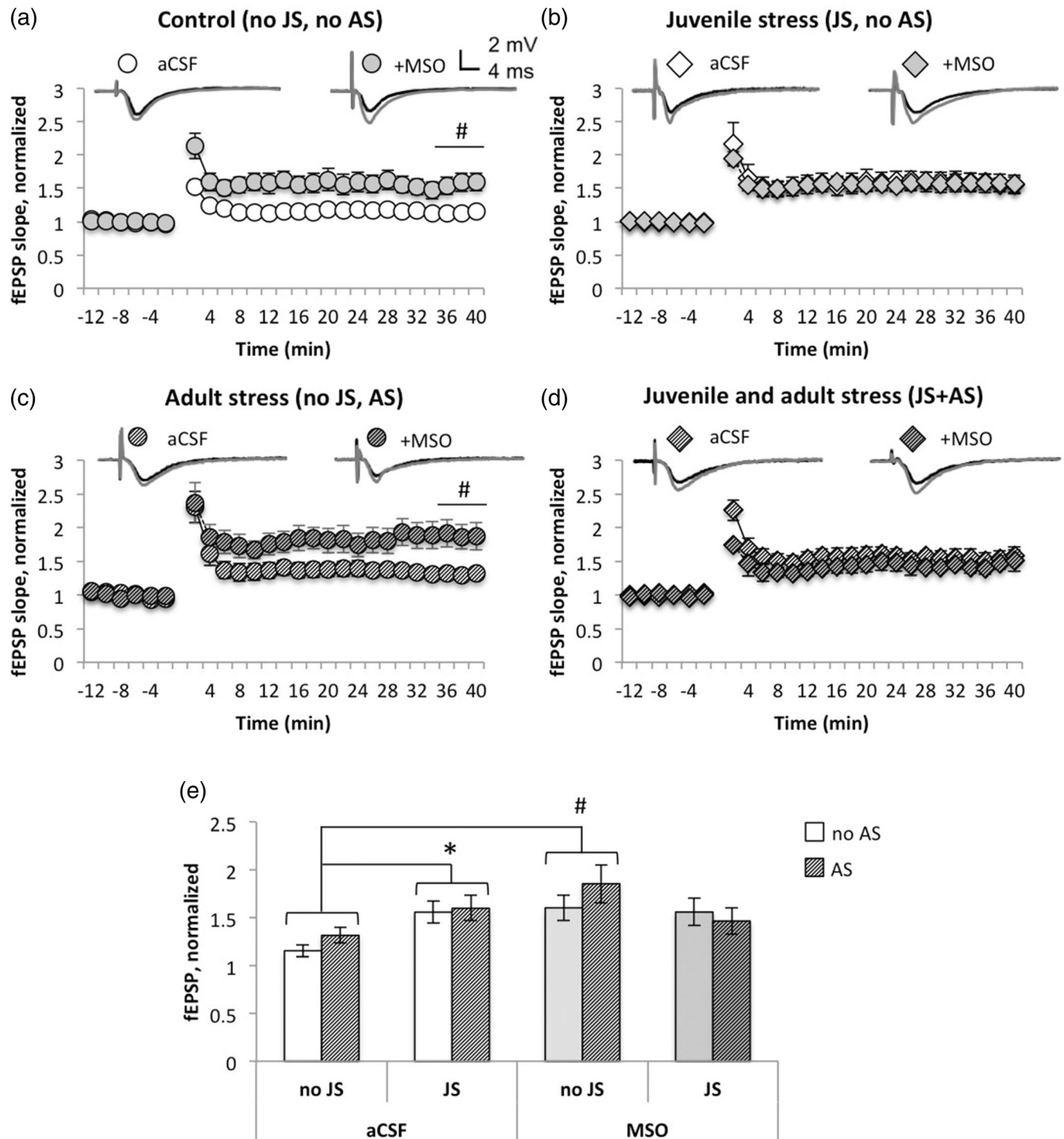


FIGURE 2 Glutamine synthetase activity is linked to stress-induced changes in long-term plasticity. Blocking the astrocytic enzyme glutamine synthetase (GS) by methionine sulfoxime (MSO) increases the long-term potentiation (LTP) in the Schaffer collateral (SC)-vCA1 synapse of slices from control animals (a, e). The effect of MSO on LTP is abolished by both juvenile stress (JS; b, e) and combined juvenile and adult stress (JSAS; d, e) where LTP is increased already in artificial cerebrospinal fluid (aCSF). However, adult stress (AS) does not affect LTP or the effect of MSO on LTP (c, e). Traces show field excitatory postsynaptic potentials (fEPSP) in the *stratum radiatum* before (black) and 40 min (gray) after high frequency stimulation (a–d). For direct comparison of all conditions, the normalized fEPSP slope is averaged over the last 5 min of recording (e). All values are mean \pm SEM. # Significant effect of MSO treatment, $p < .05$; * significant effect of JS, $p < .05$

glutamine synthetase blocker MSO induced a similar increase in LTP in slices of animals with no juvenile stress (Figure 2e: $U[42] = 2.69$, $p = .003$), but had no effect in the juvenile stress exposed group (Figure 2e: $U[43] = -0.996$, $p = .319$). The targeted comparison per stress group confirmed that MSO increased LTP in Control (Figure 2a; $U[25] = 2.33$, $p = .02$) and adult stress only animals (Figure 2c; $U[17] = 2.502$, $p = .012$) to the levels of rats with juvenile stress exposure in their history, but did not further potentiated synaptic plasticity in the vCA1 after juvenile stress alone (Figure 2b; $U[21] = -0.634$, $p = .557$) and in combination with additional adult stress (Figure 2d; $U[22] = -0.755$, $p = .45$). This suggests that a reduced function of glutamine synthetase after juvenile stress may contribute to the increased LTP observed in the vCA1 of these animals.

3.3 | Glutamine normalizes the impact of glutamine synthetase deficiency on vCA1-LTP

Accordingly, overcoming reduced GS activity by applying glutamine to the aCSF should normalize LTP also in slices of juvenile stress exposed

rats. Indeed, we observed a reduction of LTP in slices of JS-exposed rats after wash-in of 1 mM glutamine (Figure 3b,d; $U[-2.419$, $p = .015]$). While glutamine had no effect in slices from unstressed control animals (Figure 3a,d; $U[24] = -0.527$, $p = .625$), it rescued the increasing effect of MSO application on LTP in control slices (Figure 3c,d; $U[25] = -2.441$, $p = .014$). Together, our findings after glutamine wash-in further support that a functional impairment of glutamine synthetase activity critically contributes to the increased vCA1-LTP observed after juvenile stress.

3.4 | Glutamine increases synaptic efficacy after juvenile stress

The impact of glutamine wash-in was further evaluated on baseline synaptic transmission by analyzing the I-O curves (Figure 4). Glutamine (1 mM) wash-in increased the fEPSP slope in slices from naïve control animals (Figure 4a; repeated measure ANOVA with Greenhouse-Geisser correction over stimulus intensities: $F[1.656,33.126] = 3.939$, $p = .036$), but had no effect in slices of juvenile stressed animals

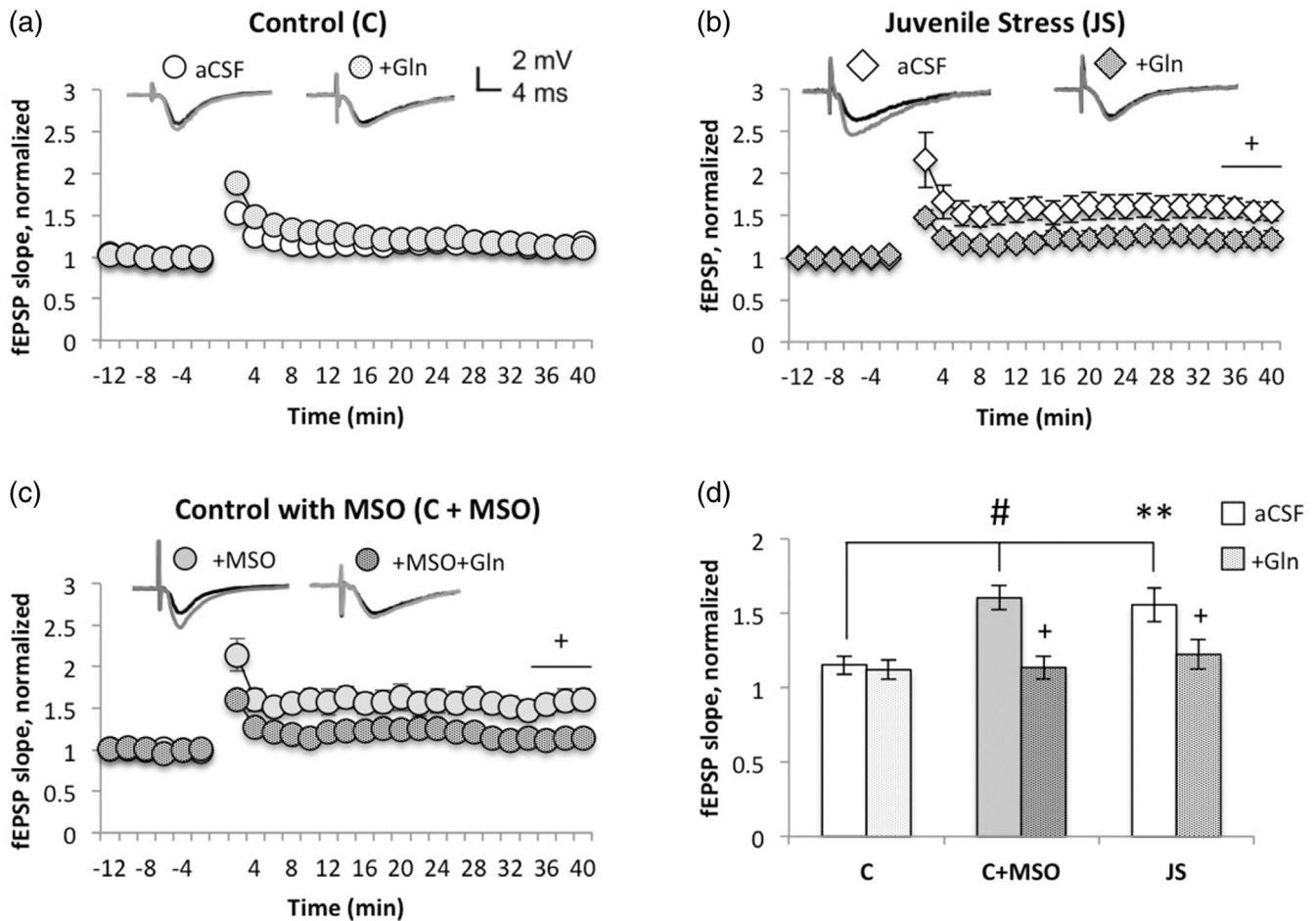


FIGURE 3 Glutamine normalizes the impact of glutamine synthetase on vCA1-LTP. While wash-in of glutamine (Gln) has no direct effect on LTP (a, d), it normalizes the enhanced vCA1-LTP observed in slices from juvenile stressed animals (b, d). Similarly, addition of glutamine prevents the increase of LTP induced by MSO in control animals (c, d). Traces show field excitatory postsynaptic potentials (fEPSP) in *stratum radiatum* before (black) and 40 min (gray) after high frequency stimulation (a–c). For direct comparison of all conditions, the normalized fEPSP slope is averaged over the last 5 min of recording (e). All values mean \pm SEM. + Significant effect of Gln treatment, $p < .05$; # significant effect of MSO treatment, $p < .05$; ** significant effect of JS exposure, $p < .01$

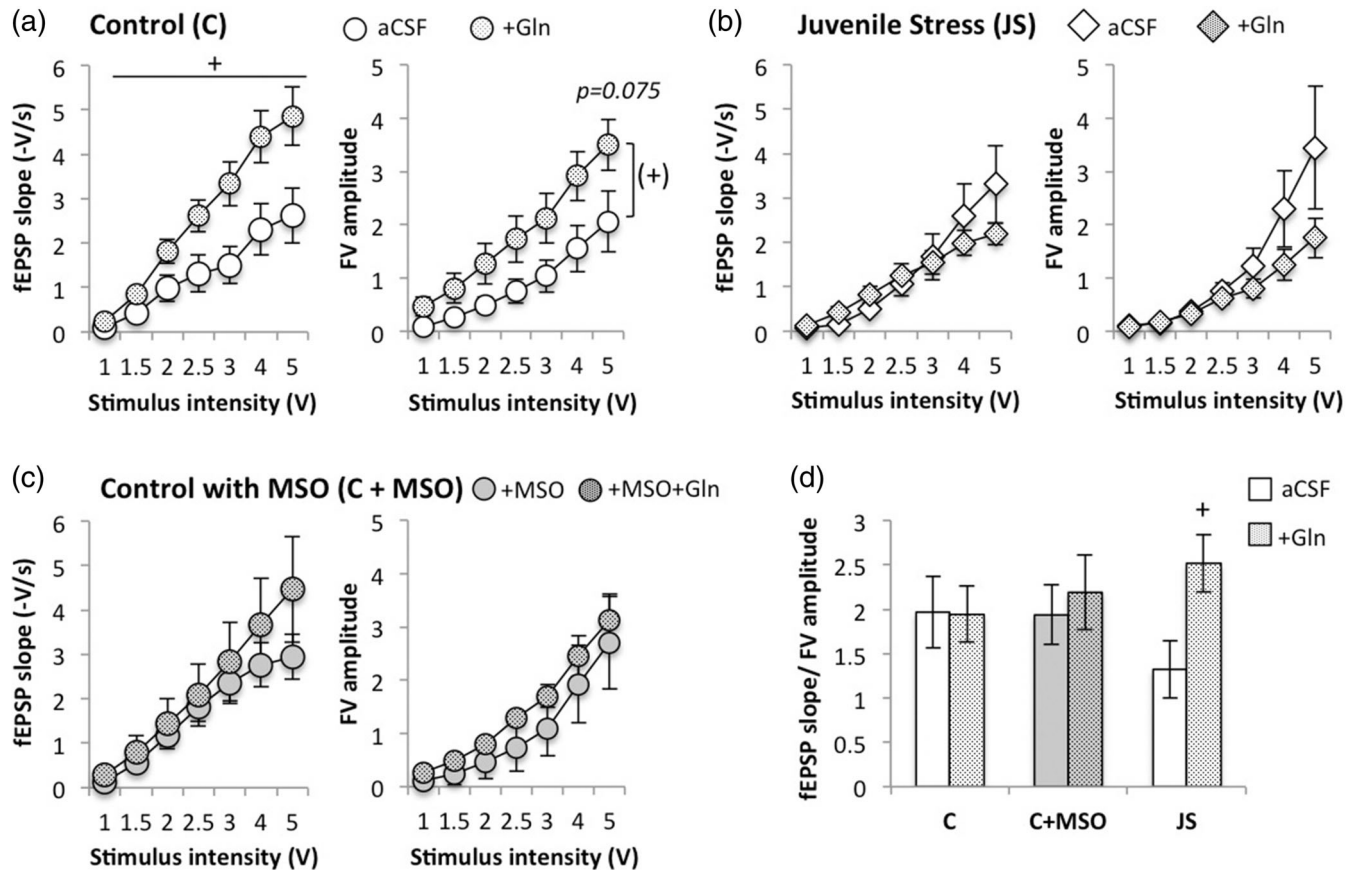


FIGURE 4 Glutamine increases synaptic efficacy after juvenile stress. Wash-in of 1 mM glutamine (Gln) increases baseline excitability in the vCA1 of control slices over increasing stimulation intensities during I–O measures, as determined by postsynaptic fEPSP slope responses and by presynaptic fiber volley amplitudes (a). No such modulation on baseline synaptic responses is observed in slices from juvenile stressed animals (b) and in control slices pretreated with MSO (c). However, glutamine elevates the synaptic efficacy (calculated as the ratio of fEPSP slope to fiber volley, averaged over all stimulation intensities) in vCA1 slices of juvenile stressed rats, but has no effect on this parameter in control slices, with and without MSO pretreatment (d). All values are mean \pm SEM. + Significant effect of Gln treatment, $p < .05$

(Figure 4b; $F[1.38,26.216] = 2.666$, $p = .104$) or after pretreatment of control slices with MSO (Figure 4c; $F[1.381,26.236] = 1.258$, $p = .288$). In trend, glutamine increased also the presynaptic stimulation response, the FV amplitude, in naïve control slices independent of the stimulation intensity (Figure 4a; main effect of glutamine: $F[1,19] = 3.554$, $p = .075$). However, when assessing the basal synaptic transmission efficacy by determining the fEPSP slope/FV amplitude ratio, glutamine wash-in had no effect in control slices but increased synaptic efficacy in slices from animals with a history of juvenile stress (Figure 4d; $F[1,14] = 6.905$). This effect was not mimicked in MSO-treated slices of control animals. Thus, the previously observed reduction of synaptic transmission efficacy by juvenile stress can be overcome by externally applied glutamine. However, this effect appears not to be directly modulated by the glutamine synthetase activity.

3.5 | Distinct regulation of steady-state mRNA levels of the glutamine–glutamate cycle after juvenile and adult stress

Following the evaluating of the functional association of GS activity and LTP effects after juvenile stress, we then tested whether a

permanent regulation of glutamine synthetase expression is observed after juvenile stress (Figure 5). To that end, mRNA expression levels for the glutamine synthetase gene (*Glu1*) as well as for other factors involved in the glutamine–glutamate cycle were determined via quantitative PCR in laser-assisted microdissected samples of the vCA1 *stratum radiatum*, the area where the Schaffer collaterals target the dendrites of CA1 pyramidal cells and LTP measurements were obtained. Two-way ANOVA for juvenile and adult stress effects revealed that expression levels of the glutamine synthetase gene were decreased by juvenile stress (Figure 5a; $F[1,24] = 4.619$, $p = .042$), but not adult stress ($F[1,24] = 3.38$, $p = .078$) and without additional significant interaction of juvenile and adult stress ($F[1,24] = 2.295$, $p = .143$). No significant main effects of juvenile stress, adult stress, or an interaction of the both were observed for the expression levels of the astrocytic glutamate uptake transporter GLT-1 (Figure 5b; juvenile stress: $F[1,24] = 0.265$, $p = .611$; adult stress: $F[1,24] = 0.679$, $p = .418$; juvenile \times adult stress: $F[1,24] = 3.595$, $p = .07$). However, a paired comparison in animals without any previous exposure to juvenile stress revealed a significantly reduced expression of GLT-1 after adult stress only ($T[12] = 2.904$, $p = .013$). Expression of the transporter responsible for shuttling glutamine from astrocytes to neurons,

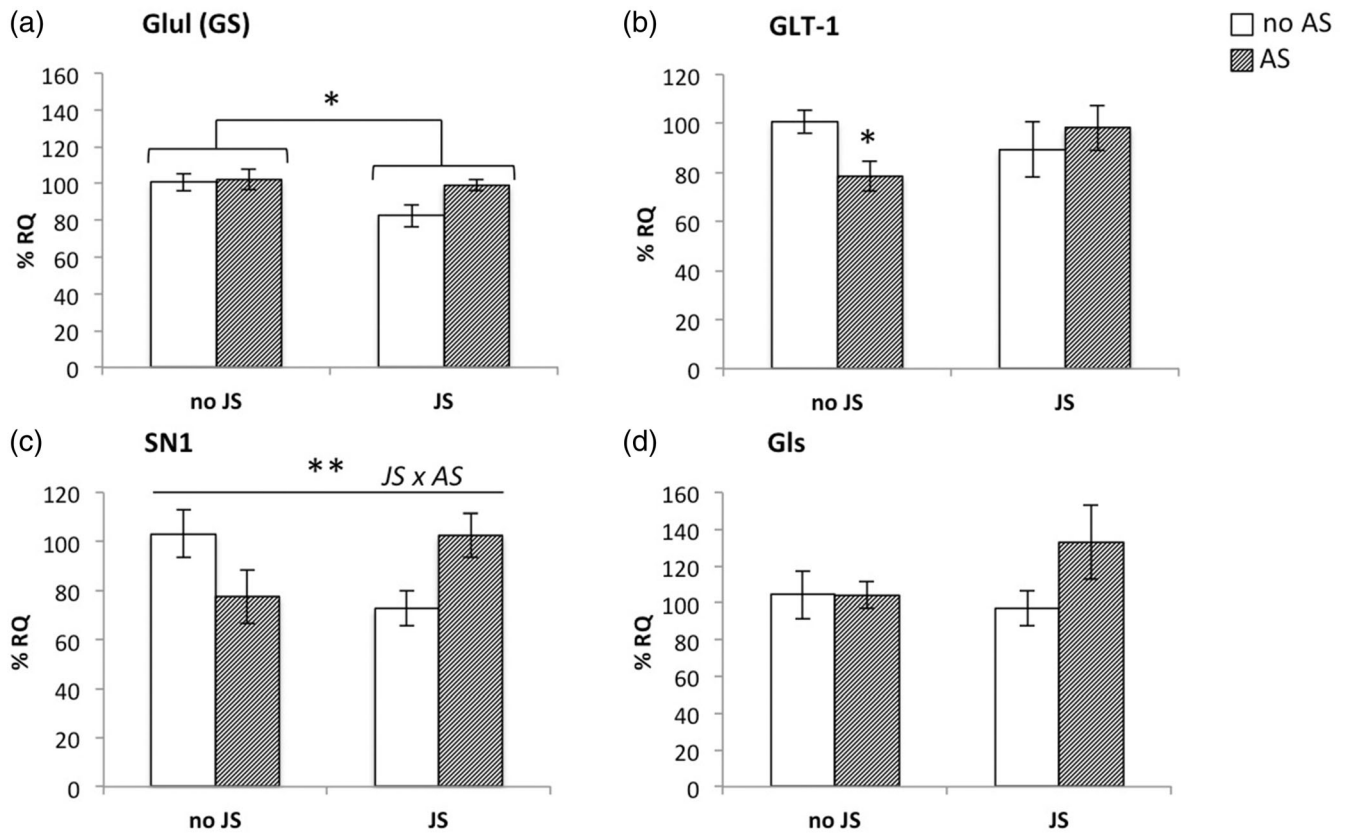


FIGURE 5 Distinct regulation of steady-state mRNA levels of the glutamine–glutamate cycle after juvenile and adult stress. Exposure to juvenile stress (JS), with and without additional adult stress (AS) induces a lasting reduction of glutamine synthetase (GluI, GS) mRNA levels in the *stratum radiatum* of the vCA1 (a). JS did not affect steady-state mRNA expression changes of the astrocytic glutamate uptake transporter GLT-1, but a single exposure of AS reduced its expression (b). No lasting shifts in the expression for glutaminase (GlS), the enzyme converting glutamine to glutamate, was observed (c). All values mean \pm SEM. * Significant effect of stress exposure groups (JS, AS, or the interaction of both, JS \times AS), $p < .05$

SN1, was reduced after single stress exposure in either juvenility or adulthood, but was restored to control levels in animals with a history of combined juvenile and adult stress (Figure 5c; juvenile stress: $F[1,25] = 0.081$, $p = .778$; adult stress: $F[1,25] = 0.046$, $p = .883$; juvenile \times adult stress: $F[1,25] = 8.528$, $p = .007$). No significant main effects or interactions were apparent for the expression levels of the glutaminase gene (GlS), the enzyme that converts glutamine to glutamate in neurons (Figure 5d; juvenile stress: $F[1,20] = 0.647$, $p = .431$; adult stress: $F[1,20] = 1.775$, $p = .198$; juvenile \times adult stress: $F[1,20] = 1.81$, $p = .194$). Based on our previous study examining the impact of juvenile stress on short and long-term plasticity in the dorsal denate gyrus (Albrecht et al., 2016), expression levels for the astrocytic GABA uptake transporter GAT-3 were analyzed as well, but no impact or juvenile or adult stress was found in the vCA1 *stratum radiatum* (Figure S2; juvenile stress: $U[28] = 0.459$, $p = .667$; adult stress: $U[28] = 0.689$, $p = .511$). Thus, expression data further may supported the role of a lastingly reduced glutamine synthetase function after juvenile stress in mediating increased LTP in the vCA1, but reveal also a complex regulation of other components of the glutamate–glutamine-cycle by stress exposure across the life span.

3.6 | Sustained glutamine synthetase protein expression levels after juvenile stress

To test whether the slight reduction in mRNA levels translates into reduced glutamine synthetase protein levels, the total number of glutamine synthetase-expressing cells as well as glutamine synthetase protein levels were assessed by glutamine synthetase immunohistochemistry, stereology, and densitometry in sections of the ventral CA1 of control and juvenile stressed rats. The number of glutamine synthetase-positive cells in the vCA1 *stratum radiatum* was not significantly reduced after juvenile stress (Figure 6c; $T[4] = 0.462$, $p = .668$). Analyzing the immunohistochemical glutamine synthetase staining intensity as a semiquantitative measure of glutamine synthetase protein expressions levels revealed no difference between vCA1 slices from control and juvenile stressed rats when comparing the dominating gray intensities (Figure 6h; $T[119] = -0.603$, $p = .548$) and the gray intensities associated with the highest pixel number (area under the curve, AUC; Figure 6i; $T[119] = -1.08$; $p = .282$). Together, protein levels of glutamine synthetase in the vCA1 *stratum radiatum* are maintained stable after juvenile stress.

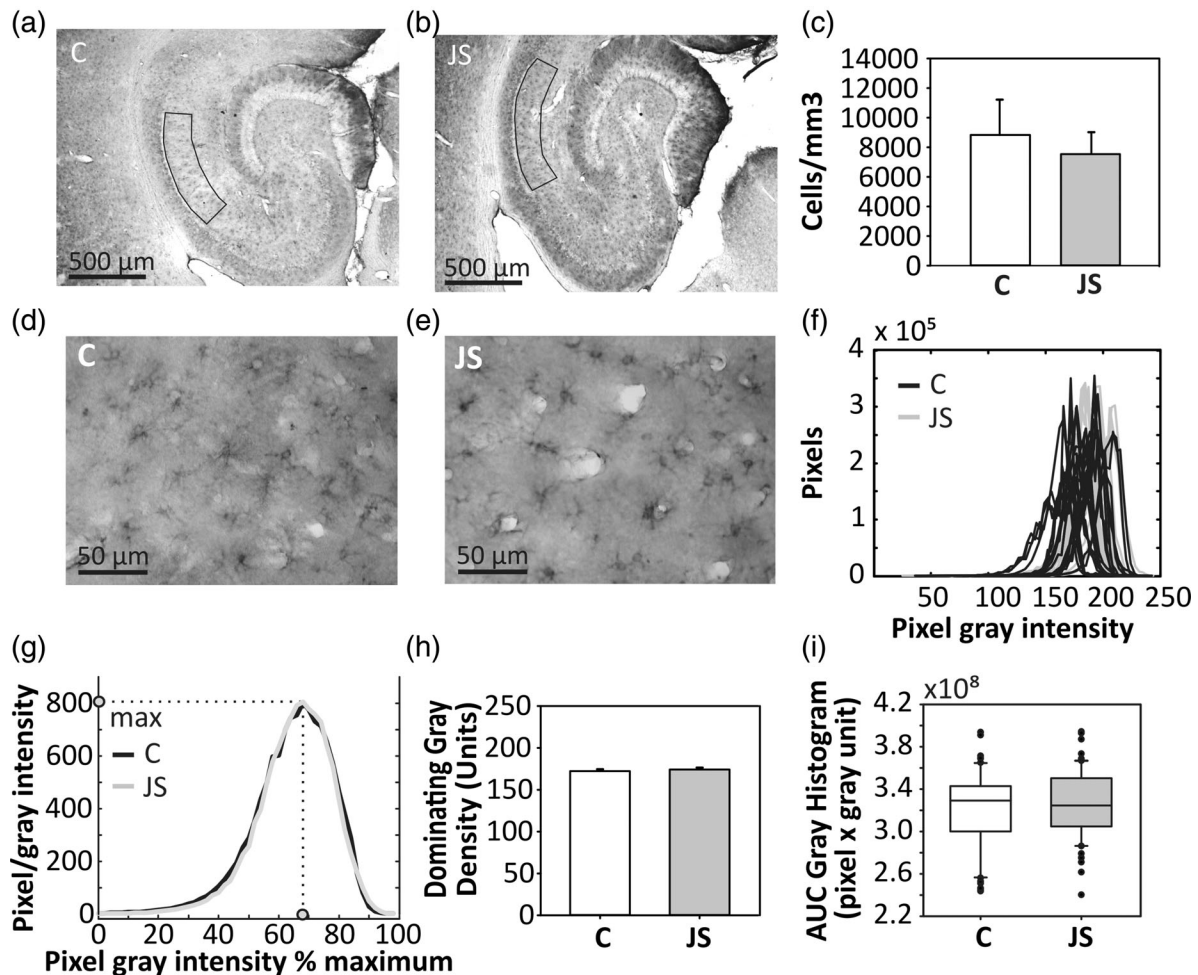


FIGURE 6 Sustained glutamine synthetase protein expression levels after juvenile stress. The number of GS expressing astrocytes as well as the intensity of protein expression was estimated in the ventral CA1 *stratum radiatum* (shaded) in 30 μm thick horizontal hippocampal slices, sample images are shown for slices from control animals (a) and slices from juvenile stress (JS) exposed rats (b). Stereology revealed no difference in the cell number density (cells/mm³) of GS-expressing astrocytes between control and JS slices (c). For the densitometric analysis of GS protein expression, ×40 microphotographs of the vCA1 *stratum radiatum* were obtained, sample images are shown from control (d) and JS rats (e). Each JS rat was stained in parallel with a randomized control and the raw gray intensity histograms of parallel-stained slices were compared, as shown for the C/JS pair of the sample images (f). Raw gray intensity histograms were normalized and averaged per group (g). No difference was spotted between histograms from the C and JS groups, measured by the dominating gray intensity (defined as the gray intensity associated with the highest pixel number; h), and by the area under the curve (AUC, i). All values mean ± SEM

4 | DISCUSSION

In the current study, we investigated the contribution of the glutamate–glutamine cycle in astrocytes on long-term alterations of plasticity in the vCA1 after juvenile stress, a rodent model for childhood adversity, and its combination with aversive learning in the two-way shuttle box serving as stress in adulthood. Subjecting rats to juvenile stress, irrespective of additional adult stress, led to a reduced basal synaptic efficacy in the vCA1, as indicated by decreased ratios of field excitatory fEPSP slope to fiber volley amplitude at Schaffer collaterals. The reduction in basal synaptic efficacy was accompanied by increased LTP after high-frequency stimulation. Notably, the impact of juvenile stress on vCA1-LTP was mimicked by a pharmacologically induced deficit of the enzyme glutamine synthetase, which converts glutamate to glutamine in astrocytes, and was rescued by

application of the glutamine synthetase product glutamine. In parallel to its lasting effects on LTP, juvenile stress also induced a slight but lasting reduction of steady state mRNA levels for the glutamine synthetase gene *Glut* in the vCA1 *stratum radiatum*. Within the same region, adult stress as well as the combination of juvenile and adult stress induced differential changes in other components of the astrocytic glutamate–glutamine cycle. However, reduced mRNA levels did not translate into reduced protein levels of glutamine synthetase in the vCA1 *stratum radiatum*, suggesting that altered glutamine synthetase turn-over and a resulting functional glutamine synthetase impairment is likely associated with increased LTP in the vCA1 after juvenile stress, with and without exposure to additional adult stress.

First, we assessed the impact of stress during juvenility and adulthood, as well as the combination of both stressors, on baseline excitability in the vCA1 Schaffer collateral synapses. Analyzing the fEPSP

slope as a measure of the postsynaptic response to increasing stimulus intensities revealed an enhanced postsynaptic excitability 2 weeks after adult stress, but a reduction if animals had a previous history of juvenile stress, while juvenile stress alone had no impact on the fEPSP slope. The presynaptic response, reflected by the FV amplitude, was not significantly altered by exposure to juvenile stress, adult stress, or the combination of both. Based on the ratio of postsynaptic fEPSP slope and presynaptic fiber volley responses upon stimulation, it is possible to assess the efficacy of synaptic transmission (Annamneedi et al., 2018; Chen et al., 2000; Nguyen et al., 2000; Patterson et al., 1996), which was reduced after juvenile stress in our experiments. Thus, for a given presynaptic stimulation (presynaptic firing) the postsynaptic response is smaller in the vCA1 of juvenile stressed animals compared to control animals. Interestingly, a reduced baseline transmission in the vCA1 was also observed in a genetic mouse model with increased anxiety and aberrant fear memory (Çaliskan et al., 2016; Winkelmann et al., 2014). Moreover, mice bred for high anxiety show a similar shift toward reduced basal synaptic transmission efficacy, along with increased LTP in the vCA1 (Dine et al., 2015), suggesting that the increase of anxiety observed after juvenile stress (Albrecht et al., 2017) may indeed be linked to reduced excitability and increased LTP in the vCA1.

In line with previous studies demonstrating an elevation of LTP in the ventral, but not dorsal CA1 region of the hippocampus as a long-term consequence of juvenile stress (Grigoryan et al., 2015; Maggio & Segal, 2011), in the current study, LTP was increased in ventral slices from animals exposed to juvenile stress. Astrocytes provide an interesting target for such a long-lasting modulation of synaptic plasticity. Recently, it was demonstrated that a chemogenetic activation of astrocytes in the hippocampal formation enhances and even induces LTP in the CA1 subregion (Adamsky et al., 2018). Multiple mechanisms how astrocytes influence synaptic plasticity have been suggested so far, including the regulation of ion homeostasis, neurovascular metabolic coupling, and gliotransmitter release (see e.g., Alberini, Cruz, Descalzi, Bessières, & Gao, 2018; Allen & Lyons, 2018; Dallérac et al., 2018, for review). Most directly, astrocytes can modulate the uptake and release rate of the neurotransmitter glutamate (Bonansco et al., 2011; Devaraju, Sun, Myers, Lauderdale, & Fiocco, 2013; Park et al., 2015; Perea & Araque, 2007), which is essential to induce LTP by binding on AMPA and NMDA receptors on the postsynaptic neuron upon strong synaptic activation (Baltaci et al., 2018; Larson & Munkácsy, 2015). Glutamate is metabolized in astrocytes to glutamine via glutamine synthetase, and glutamine is further shuttled back to neurons as a substrate for the resynthesis of glutamate (see Figure 7). Glutamine synthetase is thereby the key enzyme for this astrocytic glutamate–glutamine cycle (Rose et al., 2013). Notably, when blocking glutamine synthetase activity by MSO in control slices, we could mimic the increased vCA1-LTP observed in slices from animals with a history of juvenile stress. An additional modulatory effect of MSO was absent in slices from animals exposed to juvenile stress, but was evident in animals exposed to stress in adulthood only. These results suggest that a reduced degradation of glutamate within the astrocytic glutamate–glutamine cycle contributes to the

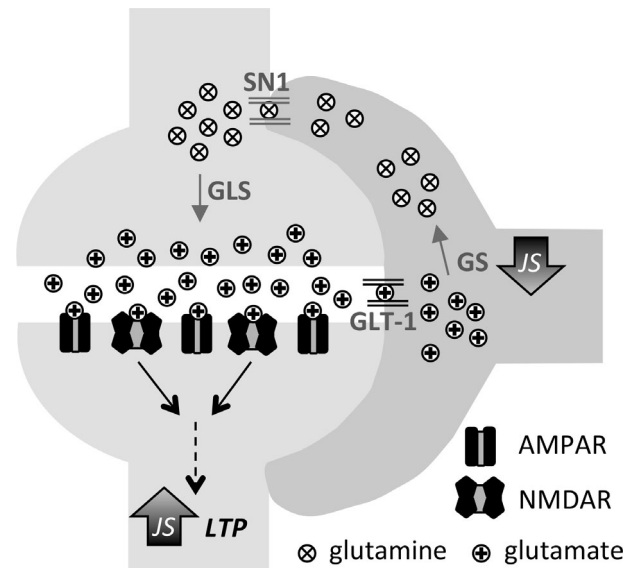


FIGURE 7 Schematic overview of our results. Upon activation of the presynaptic neuron, glutamate is released into the synaptic cleft. Astrocytes can take up glutamate from the synaptic cleft via a specific transporter, glutamate transporter 1 (GLT-1). Within astrocytes glutamate is degraded by glutamine synthetase (GS) into glutamine. Glutamine can be shuttled back to the presynaptic neuron via amino acid transporters such as SN1 (system N/Slc38a3), where it is converted to glutamate again by the enzyme glutaminase (GLS). Upon sustained stimulation of presynaptic neurons via high frequency stimulation, glutamatergic receptors of NMDA subtype are sufficiently activated on the postsynaptic site, which leads to lasting biochemical and structural changes at the synapse. These configurational changes allow for a lastingly strengthened synaptic transmission, a cellular mechanism called long-term potentiation (LTP). LTP in the vCA1 is increased by exposure to juvenile stress (JS) and is accompanied by a functional impairment of the astrocytic glutamate degrading enzyme glutamine synthetase

juvenile stress induced increase in vCA1-LTP. However, if glutamate levels were generally increased as a consequence of a functional glutamine synthetase deficiency, one would expect that MSO would modulate basal synaptic transmission as well. In our experiments, MSO neither affected basal synaptic efficacy nor the postsynaptic response measured by the fEPSP slope, in line with previous studies (Kam & Nicoll, 2007; Tani et al., 2014). The fEPSP slope was also not significantly reduced in control versus juvenile stress slices under baseline conditions, suggesting that a reduced astrocytic glutamate degradation only feeds back on the activity of glutamate transporters after high frequency stimulation, a condition where massive glutamate release occurs. This is in line with previous findings, where MSO-pretreatment to block glutamine synthetase activity indeed slows down glutamate transporters currents after high frequency stimulation, but not after low frequency stimulation in neocortical slices (Trabelsi et al., 2017). In parallel, MSO treatment also enhances NMDA receptor but not AMPA receptor mediated currents in cortical pyramidal neurons (Trabelsi et al., 2017), thereby affecting LTP but not basal synaptic transmission. Thus, after high frequency stimulation but not under baseline conditions a reduced glutamine synthetase



activity may impair glutamate clearance by glutamate transporters, allowing for induction of LTP via activation of NMDA receptors.

Applying glutamine normalized the LTP in vCA1 of juvenile stressed animals as well as in control slices that were pretreated with MSO. Substituting glutamine as the product of glutamine synthetase therefore further supports our observations of a functional glutamine synthetase deficiency in the vCA1 after juvenile stress. Glutamine, indeed, is required for maintenance of normal levels of glutamate at neuronal terminals (Laake, Slyngstad, Haug, & Ottersen, 1995) and can cause increased glutamate release in hippocampal slices (Bowyer, Lipe, Matthews, Scallet, & Davies, 1995), but also depolarizes neurons in culture (Kolbaev & Draguhn, 2008). Accordingly, it increases pre-synaptic and postsynaptic measures of basal excitability in slices of control animals in line with previous reports (Tani et al., 2014). However, synaptic efficacy was not altered under control conditions. Nevertheless, glutamine normalized the synaptic efficacy in slices of juvenile stressed rats, in parallel to its normalizing effect on LTP after juvenile stress and after MSO treatment. Indeed, glutamine concentrations are reduced by MSO treatment (Trabelsi et al., 2017), but high frequency stimulation induces a similar effect on lowering glutamine levels in vivo (Jenstad et al., 2009). Thus, assuming that juvenile stress reduces glutamine synthetase activity as well, a reduction in the glutamine supply may contribute to elevated levels of LTP. Further studies are needed to investigate how glutamine may affect LTP and its sustainment over time, including possible mechanisms affecting NMDA receptor currents or the regulation of LTP via GABAergic interneurons. Using mutant mice deficient for an interneuron-specific glutamine transporter, it has been recently demonstrated that glutamine indeed regulates GABA content and inhibitory activity of interneurons (Qureshi et al., 2019) and a decrease in inhibitory neurotransmission has been also observed after glutamine synthetase blockage with MSO in vitro (Kaczor & Mozrzymas, 2017). The resulting lowered GABAergic neurotransmission would then contribute to increased LTP via disinhibition of the vCA1 local network (Stelzer, Simon, Kovacs, & Rai, 1994). It is now tempting to speculate that similar GABAergic mechanisms also contribute to the increase in LTP observed after juvenile stress, as GABAergic mechanisms may also contribute to the behavioral phenotype induced by juvenile stress. Indeed, mice with a knock-out of the GABA-producing enzyme GAD65 show a behavioral phenotype comparable to mice and rats stressed in juvenility with increased anxiety, increased fear memory and fear generalization (see Müller, Çalışkan, & Stork, 2015 for review). Moreover, a compensatory upregulation of the expression of GABA A receptor subunits $\alpha 1$ and $\alpha 2$ was found in rats resilient to combined juvenile and adult traumatic stress exposure, while rats lacking such a regulation showed a lasting increase of anxiety-like behavior (Ardi et al., 2016).

The analysis of candidate gene mRNA expression by combining laser microdissection and subsequent qPCR provides a powerful tool to investigate subregion- and circuit-specific changes in cellular activity profiles (Albrecht et al., 2016). In fact, the analysis of steady-state mRNA levels of different components of the glutamate–glutamine cycle reveals a complex pattern of differential expression changes

induced by single juvenile or adult stress and by the combination of both stressors. We found a slight but significant chronic down-regulation of Glut mRNA, the GS gene transcript, in the vCA1 *stratum radiatum* of juvenile stressed rats. However, neither the number of glutamine synthetase-positive astrocytes nor the level of glutamine synthetase protein was reduced after juvenile stress, as assessed in the vCA1 *stratum radiatum* by immunohistochemistry in combination with stereology and densitometry. Nevertheless, the reduction of steady-state mRNA levels for the glutamine synthetase gene together with the functional deficiency derived from our pharmacological results may indicate lasting shifts in glutamine synthetase protein turn-over. A decrease of glutamine synthetase activity linked with increased degradation and a slight reduction in the new synthesis of glutamine synthetase has been also described after metabolic stress in vitro (Rosier, Lambert, & Mertens-Strijthagen, 1996) and in models of epilepsy (Papageorgiou et al., 2011). A reduction of enzymatic activity may result from oxidation and other posttranslational modifications not necessarily detected by glutamine synthetase antibodies. Hence, increased turnover in spite of apparently normal total protein levels may be associated with a reduction in active glutamine synthetase. Further, the slight reduction in glutamine synthetase gene expression observed here corresponds to the rather mild effects on basal synaptic efficacy. While glutamine synthetase total knock-out is lethal in neonates due to low glutamine and alanine cycle activity essential for metabolism (He et al., 2010), glutamine synthetase haploinsufficient mice survive but show an increased susceptibility to seizures (van Gassen, van der Hel, Hakvoort, Lamers, & de Graan, 2009). In addition, the strong reduction in glutamine synthetase activity by continuous microinfusions of MSO in the hippocampus results in recurrent seizures as well (Eid, Williamson, Lee, Petroff, & de Lanerolle, 2008), a condition usually not observed after juvenile stress.

We also screened for stress effects on the expression of the astrocytic glutamate transporter GLT-1, which takes up glutamate from the synaptic cleft into astrocytes and thereby regulates excitability (Dallérac, Chever, & Rouach, 2013). No changes in GLT-1 mRNA levels were observed after juvenile stress only, but exposure to adult stress only reduced GLT-1 expression. GLT-1 is important for balancing excitation and inhibition in the hippocampus (Héja et al., 2012). A functional reduction of GLT-1 activity therefore increases synaptic excitability, as observed in mice deficient for GLT-1 (Aida et al., 2015). Accordingly, reduced GLT-1 mRNA levels may functionally correspond to the increased baseline postsynaptic responses measured by the fEPSP slope following adult stress only (see Figure 1c). Heightened basal glutamate levels in slices of adult stress exposed animals would also allow for an increased short-term plasticity response. Indeed, directly after LTP induction by high frequency stimulation, a potentiation of the fEPSP slope was observed also in the adult stress group (see Figure 2c). However, in contrast to the juvenile stress only and the combined juvenile and adult stress group, the potentiation quickly decayed to control levels and did not last throughout our recordings (40 min after high frequency stimulation). Moreover, a total knock out of GLT-1 rather results in decreased LTP (Katagiri, Tanaka, & Manabe, 2001). Thus, the additional modulation

of GABAergic and glutamatergic neurotransmission by factors such as glutamine, as discussed above, appears to be required for increased LTP after juvenile stress. We also assessed the mRNA levels for the astrocytic glutamine transporter SN1 in the vCA1 *stratum radiatum* and found a reduction after single stress exposure episodes either in juvenility or in adulthood. When animals went through combined stress juvenile and adult stress, then SN1 mRNA expression reached again levels of control animals. A similar interaction of adult and juvenile stress effects has been observed for the basal fEPSP slope responses, which is elevated by especially adult stress, but rather reduced when adult stress follows juvenile stress pre-exposure. Glutamine release to neurons via this transporter is stimulated by activation of AMPA receptors and glutamate transporters (Todd, Marx, Hulme, Bröer, & Billups, 2017). Although speculative, it is possible that the reduced expression of the glutamate transporter GLT-1 after adult stress interacts with lowered SN1 function after juvenile stress, resulting in a normalized expression of both factors after combined juvenile and adult stress. While such a scenario may relate to altered basal synaptic transmission, shifts in SN1 expression levels after single juvenile or adult stress may not directly relate to increased LTP, as that was observed after both, juvenile stress and its combination with adult stress. However, SN1 may impact LTP in interaction with their molecular partners within the glutamate–glutamine cycle and the activity of other amino acid transporters may contribute to the observed increase in LTP after juvenile stress.

Assessing the impact of juvenile stress on plasticity within the dorsal dentate gyrus, we previously described a critical role for the transporter for taking up GABA into astrocytes, GAT-3, in regulating excitatory/inhibitory balance. Within the dorsal DG, GAT-3 mRNA and protein levels were chronically reduced, paralleled by increased inhibition during paired-pulse measurements after juvenile stress. However, neither LTP nor long-term depression was altered in the dorsal dentate gyrus (Albrecht et al., 2016). In our current analysis of the vCA1 *stratum radiatum*, no significant expression changes for GAT-3 mRNA were observed. Exposure to juvenile stress therefore appears to induce differential changes in the astrocyte-dependent modulation of short-term and long-term plasticity among different subregions of the hippocampus.

Together, we describe in this study a novel molecular correlate for increased LTP in the vCA1 as a long-term consequence of juvenile stress. A previous exposure to juvenile stress thereby leads to reduced glutamine synthetase function, the key enzyme of the astrocytic glutamine–glutamate cycle (see Figure 6 for summary). Notably, this effect is lasting for weeks. Such an effect can be viewed as an allostatic response to stress, that is, a lasting shift of plasticity in the emotional memory circuits of the brain to achieve stability or “homeostasis on a new level” (see for review: Karatsoreos & McEwen, 2011; McEwen, 2016). In our previous study, investigating the astrocytic contribution to the inhibitory/excitatory balance in the dorsal dentate gyrus, such long-term impacts on LTP were not observed (Albrecht et al., 2016). Further, the direct comparison of dorsal versus ventral hippocampus revealed an increased LTP in the ventral, but rather a decrease in the dorsal CA1 (Grigoryan et al., 2015; Maggio & Segal,

2011). The increased plasticity in the ventral hippocampus, a region linked to anxiety and emotional memory, may correspond to the lasting impact of juvenile stress on emotional behavior (Segal et al., 2010), displayed by increased anxiety and increased fear memory and its generalization in adulthood (Avital & Richter-Levin, 2005; Yee et al., 2012; Müller et al., 2014; Albrecht et al., 2017 for review). It will be interesting to assess in future studies how the ventral hippocampal GS contributes to the behavioral sequelae of juvenile stress.

ACKNOWLEDGMENTS

We are grateful to Franziska Webers for excellent technical assistance. This work was supported by the German Israeli Project Cooperation and the German Research Foundation (DIP project He1128/16-1 to UH and OS, CRC779 TPB5 to OS), the excellence cluster NeuroCure to UH, the Center for Behavioral Brain sciences Magdeburg (CBBS), supported by the European fund for regional development (EFRE), to AA (ZS/2016/04/78113) and the CBBS ScienceCampus funded by the Leibniz Association to GC (SAS-2015-LIN-LWC).

CONFLICT OF INTEREST

The authors declare no conflict of interest.

ORCID

Ismi Papageorgiou  <https://orcid.org/0000-0001-5810-0483>

Anne Albrecht  <https://orcid.org/0000-0001-8613-2968>

REFERENCES

- Adamsky, A., Kol, A., Kreisel, T., Doron, A., Ozeri-Engelhard, N., Melcer, T., ... Goshen, I. (2018). Astrocytic activation generates de novo neuronal potentiation and memory enhancement. *Cell*, *174*, 59–71.e14. <https://doi.org/10.1016/j.cell.2018.05.002>
- Aida, T., Yoshida, J., Nomura, M., Tanimura, A., Iino, Y., Soma, M., ... Tanaka, K. (2015). Astroglial glutamate transporter deficiency increases synaptic excitability and leads to pathological repetitive behaviors in mice. *Neuropsychopharmacology*, *40*, 1569–1579. <https://doi.org/10.1038/npp.2015.26>
- Alberini, C. M., Cruz, E., Descalzi, G., Bessières, B., & Gao, V. (2018). Astrocyte glycogen and lactate: New insights into learning and memory mechanisms. *Glia*, *66*, 1244–1262. <https://doi.org/10.1002/glia.23250>
- Albrecht, A., Ivens, S., Papageorgiou, I. E., Çalışkan, G., Saiepour, N., Brück, W., ... Stork, O. (2016). Shifts in excitatory/inhibitory balance by juvenile stress: A role for neuron-astrocyte interaction in the dentate gyrus. *Glia*, *64*, 911–922. <https://doi.org/10.1002/glia.22970>
- Albrecht, A., Müller, I., Ardi, Z., Çalışkan, G., Gruber, D., Ivens, S., ... Richter-Levin, G. (2017). Neurobiological consequences of juvenile stress: A GABAergic perspective on risk and resilience. *Neuroscience and Biobehavioral Reviews*, *74*, 21–43. <https://doi.org/10.1016/j.neubiorev.2017.01.005>
- Allen, N. J., & Lyons, D. A. (2018). Glia as architects of central nervous system formation and function. *Science*, *362*, 181–185. <https://doi.org/10.1126/science.aat0473>
- Annamneedi, A., Caliskan, G., Müller, S., Montag, D., Budinger, E., Angenstein, F., ... Stork, O. (2018). Ablation of the presynaptic



- organizer bassoon in excitatory neurons retards dentate gyrus maturation and enhances learning performance. *Brain Structure & Function*, 223, 3423–3445. <https://doi.org/10.1007/s00429-018-1692-3>
- Ardi, Z., Albrecht, A., Richter-Levin, A., Saha, R., & Richter-Levin, G. (2016). Behavioral profiling as a translational approach in an animal model of posttraumatic stress disorder. *Neurobiology of Disease*, 88, 139–147. <https://doi.org/10.1016/j.nbd.2016.01.012>
- Avital, A., & Richter-Levin, G. (2005). Exposure to juvenile stress exacerbates the behavioural consequences of exposure to stress in the adult rat. *The International Journal of Neuropsychopharmacology*, 8, 163–173. <https://doi.org/10.1017/S1461145704004808>
- Baltaci, S. B., Mogulkoc, R., & Baltaci, A. K. (2018). Molecular mechanisms of early and late LTP. *Neurochemical Research*, 44, 281–296. <https://doi.org/10.1007/s11064-018-2695-4>
- Bannerman, D. M., Rawlins, J. N., McHugh, S. B., Deacon, R. M., Yee, B. K., Bast, T., ... Feldon, J. (2004). Regional dissociations within the hippocampus—memory and anxiety. *Neuroscience and Biobehavioral Reviews*, 28, 273–283. <https://doi.org/10.1016/j.neubiorev.2004.03.004>
- Bonansco, C., Couve, A., Perea, G., Ferradas, C. Á., Roncagliolo, M., & Fuenzalida, M. (2011). Glutamate released spontaneously from astrocytes sets the threshold for synaptic plasticity. *The European Journal of Neuroscience*, 33, 1483–1492. <https://doi.org/10.1111/j.1460-9568.2011.07631.x>
- Bowyer, J. F., Lipe, G. W., Matthews, J. C., Scallet, A. C., & Davies, D. L. (1995). Comparison of glutamine-enhanced glutamate release from slices and primary cultures of rat brain. *Annals of the New York Academy of Sciences*, 765, 72–85 discussion 98–99.
- Çalışkan, G., Müller, I., Semtner, M., Winkelmann, A., Raza, A. S., Hollnagel, J. O., ... Meier, J. C. (2016). Identification of parvalbumin interneurons as cellular substrate of fear memory persistence. *Cerebral Cortex*, 26, 2325–2340. <https://doi.org/10.1093/cercor/bhw001>
- Chen, Q. S., Kagan, B. L., Hirakura, Y., & Xie, C. W. (2000). Impairment of hippocampal long-term potentiation by Alzheimer amyloid beta-peptides. *Journal of Neuroscience Research*, 60, 65–72. [https://doi.org/10.1002/\(SICI\)1097-4547\(20000401\)60:1<65::AID-JNR7>3.0.CO;2-Q](https://doi.org/10.1002/(SICI)1097-4547(20000401)60:1<65::AID-JNR7>3.0.CO;2-Q)
- Dalléac, G., Chever, O., & Rouach, N. (2013). How do astrocytes shape synaptic transmission? Insights from electrophysiology. *Frontiers in Cellular Neuroscience*, 7, 159. <https://doi.org/10.3389/fncel.2013.00159>
- Dalléac, G., Zapata, J., & Rouach, N. (2018). Versatile control of synaptic circuits by astrocytes: Where, when and how? *Nature Reviews. Neuroscience*, 19, 729–743. <https://doi.org/10.1038/s41583-018-0080-6>
- Devaraju, P., Sun, M. Y., Myers, T. L., Lauderdale, K., & Fiacco, T. A. (2013). Astrocytic group I mGluR-dependent potentiation of astrocytic glutamate and potassium uptake. *Journal of Neurophysiology*, 109, 2404–2414. <https://doi.org/10.1152/jn.00517.2012>
- Dine, J., Ionescu, I. A., Avrabos, C., Yen, Y. C., Holsboer, F., Landgraf, R., ... Eder, M. (2015). Intranasally applied neuropeptide S shifts a high-anxiety electrophysiological endophenotype in the ventral hippocampus towards a "normal"-anxiety one. *PLoS One*, 10, e0120272. <https://doi.org/10.1371/journal.pone.0120272>
- Eid, T., Williamson, A., Lee, T. S., Petroff, O. A., & de Lanerolle, N. C. (2008). Glutamate and astrocytes—key players in human mesial temporal lobe epilepsy? *Epilepsia*, 49(Suppl. 2), 42–52. <https://doi.org/10.1111/j.1528-1167.2008.01492.x>
- Fanselow, M. S., & Dong, H. W. (2010). Are the dorsal and ventral hippocampus functionally distinct structures? *Neuron*, 65, 7–19. <https://doi.org/10.1016/j.neuron.2009.11.031>
- Grigoryan, G., Ardi, Z., Albrecht, A., Richter-Levin, G., & Segal, M. (2015). Juvenile stress alters LTP in ventral hippocampal slices: Involvement of noradrenergic mechanisms. *Behavioural Brain Research*, 278, 559–562. <https://doi.org/10.1016/j.bbr.2014.09.047>
- Gruber, D., Gilling, K. E., Albrecht, A., Bartsch, J. C., Çalışkan, G., Richter-Levin, G., ... Behr, J. (2015). 5-HT receptor-mediated modulation of granule cell inhibition after juvenile stress recovers after a second exposure to adult stress. *Neuroscience*, 293, 67–79. <https://doi.org/10.1016/j.neuroscience.2015.02.050>
- He, Y., Hakvoort, T. B., Vermeulen, J. L., Labruyère, W. T., De Waart, D. R., Van Der Hel, W. S., ... Lamers, W. H. (2010). Glutamine synthetase deficiency in murine astrocytes results in neonatal death. *Glia*, 58, 741–754. <https://doi.org/10.1002/glia.20960>
- Heim, C., & Nemeroff, C. B. (2001). The role of childhood trauma in the neurobiology of mood and anxiety disorders: Preclinical and clinical studies. *Biological Psychiatry*, 49, 1023–1039.
- Héja, L., Nyitrai, G., Kékesi, O., Dobolyi, A., Szabó, P., Fiáth, R., ... Kardos, J. (2012). Astrocytes convert network excitation to tonic inhibition of neurons. *BMC Biology*, 10, 26. <https://doi.org/10.1186/1741-7007-10-26>
- Horovitz, O., Tsoory, M. M., Hall, J., Jacobson-Pick, S., & Richter-Levin, G. (2012). Post-weaning to pre-pubertal ('juvenile') stress: A model of induced predisposition to stress-related disorders. *Neuroendocrinology*, 95, 56–64. <https://doi.org/10.1159/000331393>
- Jenstad, M., Quazi, A. Z., Zilberter, M., Haglerød, C., Berghuis, P., Saddique, N., ... Chaudhry, F. A. (2009). System A transporter SAT2 mediates replenishment of dendritic glutamate pools controlling retrograde signaling by glutamate. *Cerebral Cortex*, 19, 1092–1106. <https://doi.org/10.1093/cercor/bhn151>
- Kaczor, P. T., & Mozrzymas, J. W. (2017). Key metabolic enzymes underlying astrocytic upregulation of GABAergic plasticity. *Frontiers in Cellular Neuroscience*, 11, 144. <https://doi.org/10.3389/fncel.2017.00144>
- Kam, K., & Nicoll, R. (2007). Excitatory synaptic transmission persists independently of the glutamate-glutamine cycle. *The Journal of Neuroscience*, 27, 9192–9200. <https://doi.org/10.1523/JNEUROSCI.1198-07.2007>
- Karatsoreos, I. N., & McEwen, B. S. (2011). Psychobiological allostasis: Resistance, resilience and vulnerability. *Trends in Cognitive Sciences*, 15, 576–584. <https://doi.org/10.1016/j.tics.2011.10.005>
- Katagiri, H., Tanaka, K., & Manabe, T. (2001). Requirement of appropriate glutamate concentrations in the synaptic cleft for hippocampal LTP induction. *The European Journal of Neuroscience*, 14, 547–553.
- Kolbaev, S., & Draguhn, A. (2008). Glutamine-induced membrane currents in cultured rat hippocampal neurons. *The European Journal of Neuroscience*, 28, 535–545. <https://doi.org/10.1111/j.1460-9568.2008.06365.x>
- Koolhaas, J. M., Bartolomucci, A., Buwalda, B., de Boer, S. F., Flügge, G., Korte, S. M., ... Fuchs, E. (2011). Stress revisited: A critical evaluation of the stress concept. *Neuroscience and Biobehavioral Reviews*, 35, 1291–1301. <https://doi.org/10.1016/j.neubiorev.2011.02.003>
- Laake, J. H., Slyngstad, T. A., Haug, F. M., & Ottersen, O. P. (1995). Glutamine from glial cells is essential for the maintenance of the nerve terminal pool of glutamate: Immunogold evidence from hippocampal slice cultures. *Journal of Neurochemistry*, 65, 871–881.
- Larson, J., & Munkácsy, E. (2015). Theta-burst LTP. *Brain Research*, 1621, 38–50. <https://doi.org/10.1016/j.brainres.2014.10.034>
- Maggio, N., & Segal, M. (2011). Persistent changes in ability to express long-term potentiation/depression in the rat hippocampus after juvenile/adult stress. *Biological Psychiatry*, 69, 748–753. <https://doi.org/10.1016/j.biopsych.2010.11.026>
- McEwen, B. S. (2016). In pursuit of resilience: Stress, epigenetics, and brain plasticity. *Annals of the New York Academy of Sciences*, 1373, 56–64. <https://doi.org/10.1111/nyas.13020>
- McLaughlin, K. A., Kubzansky, L. D., Dunn, E. C., Waldinger, R., Vaillant, G., & Koenen, K. C. (2010). Childhood social environment, emotional reactivity to stress, and mood and anxiety disorders across the life course. *Depression and Anxiety*, 27, 1087–1094. <https://doi.org/10.1002/da.20762>
- Müller, I., Çalışkan, G., & Stork, O. (2015). The GAD65 knock out mouse - a model for GABAergic processes in fear- and stress-induced psychopathology. *Genes, Brain, and Behavior*, 14, 37–45. <https://doi.org/10.1111/gbb.12188>
- Müller, I., Obata, K., Richter-Levin, G., & Stork, O. (2014). GAD65 haploinsufficiency conveys resilience in animal models of stress-induced

- psychopathology. *Frontiers in Behavioral Neuroscience*, 8, 265–1094. <https://doi.org/10.1002/da.20762>
- Nguyen, P. V., Abel, T., Kandel, E. R., & Bourtoouladze, R. (2000). Strain-dependent differences in LTP and hippocampus-dependent memory in inbred mice. *Learning & Memory*, 7, 170–179.
- Papageorgiou, I. E., Gabriel, S., Fetani, A. F., Kann, O., & Heinemann, U. (2011). Redistribution of astrocytic glutamine synthetase in the hippocampus of chronic epileptic rats. *Glia*, 59, 1706–1718. <https://doi.org/10.1002/glia.21217>
- Park, H., Han, K. S., Seo, J., Lee, J., Dravid, S. M., Woo, J., ... Lee, C. J. (2015). Channel-mediated astrocytic glutamate modulates hippocampal synaptic plasticity by activating postsynaptic NMDA receptors. *Molecular Brain*, 8, 7. <https://doi.org/10.1186/s13041-015-0097-y>
- Patterson, S. L., Abel, T., Deuel, T. A., Martin, K. C., Rose, J. C., & Kandel, E. R. (1996). Recombinant BDNF rescues deficits in basal synaptic transmission and hippocampal LTP in BDNF knockout mice. *Neuron*, 16, 1137–1145.
- Paxinos, G., & Watson, C. (1998). *The rat brain: In stereotaxic coordinates* (2nd ed.). San Diego, CA: Academic Press.
- Perea, G., & Araque, A. (2007). Astrocytes potentiate transmitter release at single hippocampal synapses. *Science*, 317, 1083–1086. <https://doi.org/10.1126/science.1144640>
- Qureshi, T., Sørensen, C., Berghuis, P., Jensen, V., Dobszay, M. B., Farkas, T., ... Chaudhry, F. A. (2019). The glutamine transporter Slc38a1 regulates GABAergic neurotransmission and synaptic plasticity. *Cerebral Cortex*, bhz055. <https://doi.org/10.1093/cercor/bhz055>
- Rose, C. F., Verkhratsky, A., & Parpura, V. (2013). Astrocyte glutamine synthetase: Pivotal in health and disease. *Biochemical Society Transactions*, 41, 1518–1524. <https://doi.org/10.1042/BST20130237>
- Rosier, F., Lambert, D., & Mertens-Strijthagen, M. (1996). Effect of glucose deprivation on rat glutamine synthetase in cultured astrocytes. *The Biochemical Journal*, 315, 607–612. <https://doi.org/10.1042/bj3150607>
- Segal, M., Richter-Levin, G., & Maggio, N. (2010). Stress-induced dynamic routing of hippocampal connectivity: A hypothesis. *Hippocampus*, 20, 1332–1338. <https://doi.org/10.1002/hipo.20751>
- Stelzer, A., Simon, G., Kovacs, G., & Rai, R. (1994). Synaptic disinhibition during maintenance of long-term potentiation in the CA1 hippocampal subfield. *Proceedings of the National Academy of Sciences of the United States of America*, 91, 3058–3062. <https://doi.org/10.1073/pnas.91.8.3058>
- Tani, H., Dulla, C. G., Farzampour, Z., Taylor-Weiner, A., Huguenard, J. R., & Reimer, R. J. (2014). A local glutamate-glutamine cycle sustains synaptic excitatory transmitter release. *Neuron*, 81, 888–900. <https://doi.org/10.1016/j.neuron.2013.12.026>
- Todd, A. C., Marx, M. C., Hulme, S. R., Bröer, S., & Billups, B. (2017). SNAT3-mediated glutamine transport in perisynaptic astrocytes in situ is regulated by intracellular sodium. *Glia*, 65, 900–916. <https://doi.org/10.1002/glia.23133>
- Trabelsi, Y., Amri, M., Becq, H., Molinari, F., & Anikstejn, L. (2017). The conversion of glutamate by glutamine synthase in neocortical astrocytes from juvenile rat is important to limit glutamate spillover and peri/extrasynaptic activation of NMDA receptors. *Glia*, 65, 401–415. <https://doi.org/10.1002/glia.23099>
- van Gassen, K. L., van der Hel, W. S., Hakvoort, T. B., Lamers, W. H., & de Graan, P. N. (2009). Haploinsufficiency of glutamine synthetase increases susceptibility to experimental febrile seizures. *Genes, Brain, and Behavior*, 8, 290–295. <https://doi.org/10.1111/j.1601-183X.2008.00471.x>
- Winkelmann, A., Maggio, N., Eller, J., Caliskan, G., Semtner, M., Häussler, U., ... Meier, J. C. (2014). Changes in neural network homeostasis trigger neuropsychiatric symptoms. *The Journal of Clinical Investigation*, 124, 696–711. <https://doi.org/10.1172/JCI71472>
- Yee, N., Schwarting, R. K., Fuchs, E., & Wöhr, M. (2012). Juvenile stress potentiates aversive 22-kHz ultrasonic vocalizations and freezing during auditory fear conditioning in adult male rats. *Stress*, 15, 533–544. <https://doi.org/10.3109/10253890.2011.646348>

SUPPORTING INFORMATION

Additional supporting information may be found online in the Supporting Information section at the end of this article.

How to cite this article: Ivens S, Çalışkan G, Papageorgiou I, et al. Persistent increase in ventral hippocampal long-term potentiation by juvenile stress: A role for astrocytic glutamine synthetase. *Glia*. 2019;67:2279–2293. <https://doi.org/10.1002/glia.23683>